

Engineering Notes

ENGINEERING NOTES are short manuscripts describing new developments or important results of a preliminary nature. These Notes cannot exceed 6 manuscript pages and 3 figures; a page of text may be substituted for a figure and vice versa. After informal review by the editors, they may be published within a few months of the date of receipt. Style requirements are the same as for regular contributions (see inside back cover).

Adaptive Shunting for Vibration Control of Frequency-Varying Structures

Keun-Ho Rew* and In Lee†

Korea Advanced Institute of Science and Technology,
Taejon 305-701, Republic of Korea

Introduction

FEW passive shunt circuits connected to piezoelectric ceramics can be used to successfully suppress vibrations in structures. However, the performance of a passive shunt circuit optimally tuned at some specific natural frequency of a base structure will deteriorate as that frequency changes. Frequency changes often occur in structures such as robot manipulators with arbitrary payloads and space structures with deployable antennas. An adaptive shunt circuit with a multiplier integrated circuit (IC) has been developed to overcome this problem.

Hagood and von Flotow¹ formulated the coupled piezoelectric-structure equations and found formulas for the optimal parameters of the shunt circuit. Aldrich et al.² used piezoelectric ceramics weighting only 0.5 kg total and passive shunt circuits to control Advanced Space Structures Technology Research Experiment, a 5-ton structure. They obtained a good control performance. Hollkamp³ adopted the synthetic inductance and showed that the inductance, resistance, and capacitance connected in serial (L–R–C) network circuit shunted with one piezoelectric ceramic can suppress multimodal vibrations. Hollkamp and Starchville⁴ also proposed a self-tuning passive shunting with a motorized potentiometer. They used a direct adaptive control method and a least-mean-squares technique to adjust the motorized potentiometer. Rew et al.⁵ proposed the adaptive positive position feedback method to estimate the natural frequencies in real time and to suppress the multimodal vibrations of a frequency-varying composite plate.

In the present study, the method proposed by Hollkamp and Starchville⁴ is improved on, and an adaptive shunt circuit is proposed. First, an equivalent resistance circuit using a multiplier IC (number AD633) replaces the motorized potentiometer. Second, a digital signal processing (DSP) board estimates the natural frequency of a composite beam using the recursive least square (RLS) method⁵ and computes the command voltage to adjust the adaptive shunt circuit in real time. The proposed adaptive shunt circuit is relatively simple and economical and consumes less power (600 mW) than the motorized potentiometer method (5–10 W). The bandwidth of the proposed circuit is increased from 100 Hz to 1 MHz. The characteristics of the adaptive shunt circuit are analyzed and observed experimentally.

Received 2 October 2000; revision received 7 July 2001; accepted for publication 14 July 2001. Copyright © 2001 by the American Institute of Aeronautics and Astronautics, Inc. All rights reserved.

*Graduate Research Assistant, Department of Aerospace Engineering, Student Member AIAA.

†Professor, Department of Aerospace Engineering, Senior Member AIAA.

Theory on Passive and Adaptive Shunting

Generally, resonant shunted piezoelectric (RSP) shunting (resonant shunting) is more effective than resistive shunting. RSP shunting, a form of passive shunting, is discussed in this study.

The nondimensional mechanical impedance of a passive shunt circuit can be given as^{1,3}

$$\bar{Z}_{jj}^{\text{RSP}}(s) = 1 - k_{ij}^2 [\delta^2 / (\gamma^2 + \delta^2 r \gamma + \delta^2)] \quad (1)$$

where k_{ij} is the electromechanical coupling factor of the piezoelectric material; $\gamma (= s/\omega_n^E)$ is the nondimensional frequency; s is the Laplace parameter; ω_n^E is the natural frequency of the structural mode when the circuit is shorted; $r (= R_0 C_p^S \omega_n^E)$ denotes the electrical damping factor; R_0 is the resistance of the shunt circuit; C_p^S is the capacitance of the piezoelectric material; $\omega_e [= 1/\sqrt{(L_{\text{eq}} C_p^S)}]$ is the electrical resonance frequency; L_{eq} is the equivalent inductance synthesized with operational amps, capacitance, and resistances; and $\delta (= \omega_e/\omega_n^E)$ is the normalized electrical resonant frequency, which is a critical tuning parameter.

Tuning by the transfer function (TF) method is introduced here to maximize the dissipation of the vibration energy^{1,3}:

$$\delta_{\text{TF}}^{\text{opt}} = \sqrt{1 + K_{ij}^2}, \quad r_{\text{TF}}^{\text{opt}} \cong \sqrt{2} K_{ij} / (1 + K_{ij}^2) \quad (2)$$

where ω_n^D is the natural frequency of the structural mode when the circuit is opened and $K_{ij}^2 = \{(\omega_n^D)^2 - (\omega_n^E)^2\} / (\omega_n^E)^2$ is the generalized coupling factor.

We will now discuss adaptive shunting. The configuration of an adaptive shunt circuit is shown in Fig. 1. The dashed rectangular area represents the equivalent inductance.^{3,4} The multiplier IC gives adjustability to the circuit. The resonant frequency of this circuit can be changed with the command voltage. This is the essence of adaptive shunting. The multiplier amplifies the sensing and command voltages and generates an offset voltage. Thus, the current on the upper R_1 is derived. The equivalent resistance R_{eq} is given as follows:

$$R_{\text{eq}} = V_a / i = R_1 / (1 - 0.1 \cdot V_c) \quad (3)$$

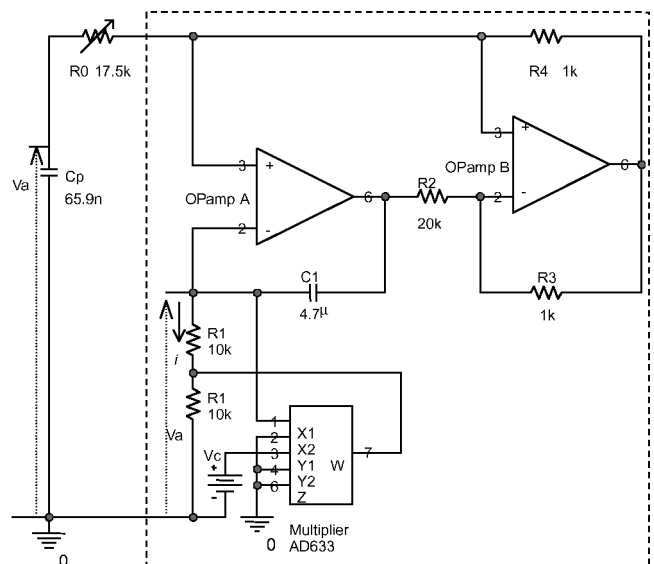


Fig. 1 Configuration of adaptive shunt circuit.

When the resistance R_3 is equal to the resistance R_4 , the synthetic inductance can be obtained from Eq. (3), as follows:

$$L_{eq} = (R_4/R_3)R_2C_1R_{eq} = R_2C_1R_{eq} = R_2C_1[R_1/(1 - 0.1 \cdot V_c)] \quad (4)$$

Considering $\delta = \omega_e/\omega_n^E$, we can obtain the relation between the command voltage and the natural frequency of a composite beam from Eq. (4), as follows:

$$V_c = 10 \cdot [1 - R_1C_1R_2C_p^S(\delta \cdot \omega_n^E)^2] \quad (5)$$

Experimental Procedures and Results

A graphite/epoxy composite beam is manufactured, and the layer angle of the composite beam is $[0_2/90_2]_s$. A band-limited white disturbance generated from the fast Fourier transform (FFT) analyzer is fed into the magnetic transducer, and electromagnetic force excites the beam. The response of the beam is measured using the laser displacement sensor. The measured signal is fed into the DSP board, and then the natural frequency is estimated using the RLS method in real time. The DSP board estimates the natural frequency and computes the command voltage for the adaptive shunt circuit.

Figure 2 shows the frequency responses of the adaptive shunt circuit obtained using Eq. (1). The S and T points are monitored following a procedure recommended in Ref. 1. Using the experimental tuning, we obtained the tuned parameters for the passive and the adaptive shunting: $\delta_p = 1.0094$, $r_p = 0.08966$, $\delta_a = 1.0089$, and $r_a = 0.08966$. The subscripts p and a refer to the passive and the adaptive shunting, respectively.

The RLS method⁵ was used to estimate the natural frequency in real time. F0, F1, and F2, given in Fig. 3, denote the cases without additional mass and with one and two additional masses at the beam tip, respectively. The sampling time is 5 ms, which is small enough to prevent aliasing. The DSP board estimates the natural frequency and computes the command voltage within the sampling time. The forgetting factor for the RLS method is set at 0.998, which was found to provide a good compromise between robustness to noise and convergence speed.

In each case, the estimated natural frequency converges accurately to the actual experimental results obtained by the FFT analyzer using eight ensemble averages, although the experimental results for frequency estimation are not presented in this Note.

The natural frequencies are 23 and 35% lower in the F1 and F2 cases than in the F0 case, respectively. The passive shunting attenuates the vibrations by 21.56, 4.55, and 0.35 dB in the F0, F1, and F2 cases, respectively, as shown in Fig. 3a. As shown in Fig. 3a, the control performance of passive shunting is not very high when the natural frequency of the structure changes.

On the contrary, the adaptive shunting successfully reduces the vibrations by 22.3, 22.1, and 20.6 dB, as shown in Fig. 3b. The performance of the adaptive shunting is excellent compared to that of the passive shunting.

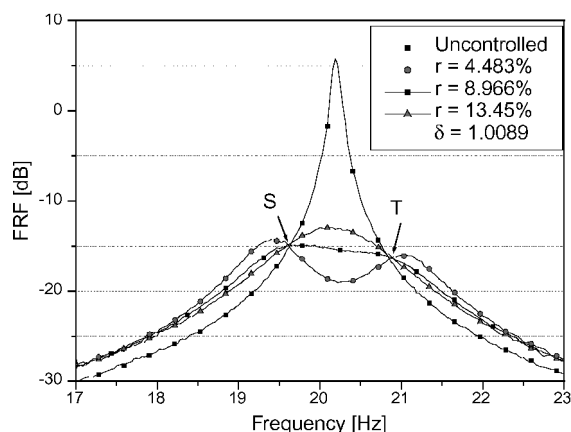
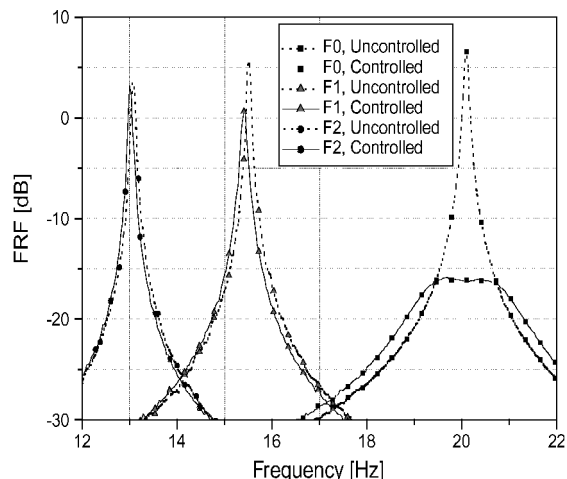
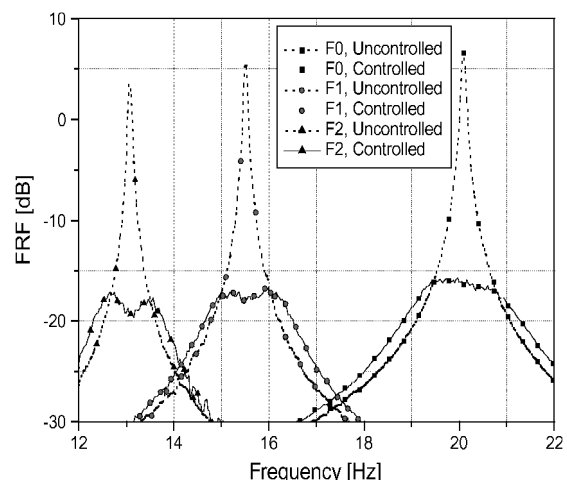


Fig. 2 Tuning characteristics of adaptive shunt circuit.



a) Passive shunting



b) Adaptive shunting

Fig. 3 Vibration control results with passive and adaptive shunting.

Conclusions

To overcome the performance degradation of passive shunting when the natural frequency of a structure changes, adaptive shunting using a multiplier IC is proposed and successfully demonstrated.

The experimental results indicate that the adaptive shunt circuit has the same tuning characteristics as the passive shunt circuit. The RLS method is used to estimate the natural frequency of the beam in real time. With the estimated natural frequency, the command voltage adjusts the adaptive shunt circuit to track the frequency variation, and the vibration was reduced by 20 dB with the adaptive shunting for a 35% change in the natural frequency. On the contrary, the same frequency change drastically degraded the performance of the passive shunting. The proposed adaptive shunting can reduce vibration successfully in the presence of changes in the natural frequency of the base structure.

Acknowledgments

The authors gratefully acknowledge the support (Subject 2000-N-NL-01-C-250) of the National Research Laboratory Program of the Ministry of Science and Technology, Republic of Korea, and wish to express special appreciation to Sung-Hun Woo of the Korean Advanced Institute of Science and Technology, who provided useful comments.

References

- Hagood, N. W., and von Flotow, A., "Damping of Structural Vibrations with Piezoelectric Materials and Passive Electrical Networks," *Journal of Sound and Vibration*, Vol. 146, No. 2, 1991, pp. 243–268.
- Aldrich, J. B., Hagood, N. W., von Flotow, A., and Vos, D. W., "Design of Passive Piezoelectric Damping for Space Structures," *Proc. SPIE*, Vol. 1917, 1993, pp. 692–705.

³Hollkamp, J. J., "Multimodal Passive Vibration Suppression with Piezoelectrics," AIAA Paper 93-1683, 1993.

⁴Hollkamp, J. J., and Starchville, T. F., "A Self-Tuning Piezoelectric Vibration Absorber," *Journal of Intelligent Materials Systems and Structures*, Vol. 5, No. 4, 1994, pp. 559–566.

⁵Rew, K.-H., Han, J. H., and Lee, I., "Adaptive Multimodal Vibration Control of Winglike Composite Structure Using Adaptive Positive Position Feedback," AIAA Paper 2000-1422, 2000.

Level Flight Trim and Stability Analysis Using Extended Bifurcation and Continuation Procedure

N. Ananthkrishnan* and Nandan K. Sinha†

Indian Institute of Technology, Bombay 400 076, India

I. Introduction

AIRCRAFT that are designed for rapid maneuvering and for controlled flight at high angles of attack often experience a variety of flight instabilities, that result in nonlinear phenomena, such as wing rock and spin, or in loss-of-control problems, such as yaw departure. The bifurcation and continuation method is the standard tool in use today for the analysis and prediction of flight instability phenomena. The standard bifurcation analysis (SBA) procedure can be used to study any dynamic system of the following form:

$$\dot{\mathbf{x}} = \mathbf{f}(\mathbf{x}, u, \mathbf{p}) \quad (1)$$

where \mathbf{x} is the vector of state variables, u is the control parameter being varied, and \mathbf{p} is the vector of parameters kept fixed. The equations for rigid aircraft flight dynamics (see the Appendix) appear as a set of eight first-order differential equations of precisely the form of Eq. (1), with a typical choice of states, control parameter, and fixed parameters, as follows:

$$\mathbf{x} = [M, \alpha, \beta, p, q, r, \phi, \theta], \quad u = \delta e, \quad \mathbf{p} = [\eta, \delta a, \delta r]$$

where M is the Mach number, η is the throttle as a fraction of maximum thrust, and the other variables have their standard meanings. Thus, the SBA procedure can be directly applied to the aircraft flight dynamic equations in the Appendix. When a starting trim condition $(\mathbf{x}_0, u_0, \mathbf{p}_0)$ is given, the SBA procedure uses a continuation algorithm to compute the entire branch of trim states \mathbf{x} with varying values of the control u , but with \mathbf{p}_0 held fixed. The continuation algorithm also calculates the Jacobian matrix of the dynamic system Eq. (1) at each trim, which is used to indicate the stability of that trim. Bifurcation points along the trim branch can be located, and bifurcating solution branches such as limit cycles can be tracked by the SBA procedure. The SBA procedure has been employed in this manner to study the onset of flight instabilities such as wing rock, spiral divergence, and spin and also to devise recovery strategies from difficult flight conditions such as spin, to prevent undesirable phenomena such as jump in roll maneuvers, and as an aid to control law design.^{1–4} A detailed introduction to the SBA procedure has been provided by Goman et al.⁵

The different trims along a branch computed by the SBA procedure do not, in general, share a common value of a state variable

such as angle of attack or Mach number. For example, when the SBA procedure is started with a level flight trim and the elevator is used as the control, it is seen that other computed trims along the branch do not correspond to level flight. However, there are several reasons for desiring the bifurcation analysis procedure to be able to constrain one or more states to their values at the starting point. A bifurcation analysis procedure that can account for state variable constraints could be used to evaluate aircraft performance parameters such as the maximum roll rate in zero-sideslip roll maneuvers, or the maximum turn rate in a level turn. The ability to generate successive trim states, all satisfying a common level flight condition, would be a useful input to control law design. Also, a bifurcation analysis that can handle state constraints may be expected to show results that correlate better with flight tests because it can be used to reproduce maneuvers flown by pilots. A constrained bifurcation analysis (CBA) procedure was first used by Ananthkrishnan and Sudhakar⁶ to study roll maneuvers with a zero-sideslip constraint, followed by a study of velocity vector roll maneuvers by Modi and Ananthkrishnan.⁷ The CBA procedure and its application to level flight maneuvers has been described in a recent paper by Pashilkar and Pradeep.⁸ The CBA procedure requires the constraint equations to be appended to the equations for the aircraft dynamics, giving an augmented set of state plus constraint equations, as follows:

$$\dot{\mathbf{x}} = \mathbf{f}(\mathbf{x}, u, \mathbf{p}), \quad \mathbf{y} = \mathbf{g}(\mathbf{x}) = 0 \quad (2)$$

where \mathbf{g} is an m -dimensional vector function that represents the constraints. Let \mathbf{x} have dimension n . Then, to use a continuation algorithm with the set of $(n + m)$ equations in Eq. (2), it is necessary to have $(n + m + 1)$ variables or unknowns. Clearly, the additional m variables must be obtained from the parameter vector \mathbf{p} . Therefore, as many elements of \mathbf{p} are freed as there are constraint equations in the augmented set, so that the CBA problem is well posed. A continuation algorithm is then used to compute the trim states along with the values of the freed parameters as a function of the control u . All such computed trims naturally satisfy the imposed constraint, and the computed values of the freed parameters indicate how they should be varied in practice with the control u , to achieve the demanded constraints.

However, the CBA procedure is unsatisfactory in two respects. First, the CBA procedure with the augmented set of equations in Eq. (2) does not provide correct information about the stability of the trim points. This is because present continuation algorithms internally compute the Jacobian of the augmented set of equations, where they regard the constraint equations at par with the state equations. The eigenvalues computed from the augmented Jacobian matrix do not correctly reflect the stability of the constrained trim state. This may be regarded more as a limitation of the continuation software than a shortcoming of the CBA procedure. However, previous attempts to overcome this problem required either numerical simulations or extraction and separate computation of the appropriate submatrix of the Jacobian matrix at each trim point, both procedures being tedious and inefficient. Second, as part of the CBA procedure, it is of interest to identify possible departures from the constrained flight condition, which may be expected when the constrained trim states lose stability. The CBA procedure, however, cannot compute solutions that depart from the constraints because the analysis always includes the constraint equations. Informally speaking, in the CBA procedure, the constraints are always on, hence, only trims that obey the constraints are computed. Thus, previous attempts at carrying out bifurcation analysis in the presence of constraints have been hampered by the inability of the CBA procedure to extract stability information from the continuation algorithm and its inability to trace departures from the constrained trim states.

In this Note, we propose a new method called the extended bifurcation and continuation procedure that overcomes these drawbacks of the CBA procedure. The extended bifurcation analysis (EBA) procedure, in the presence of state variable constraints, computes trim points satisfying the constraints along with their correct stability and tracks departures from the constrained flight at points where the trim states lose stability. Thus, it becomes possible to generate complete bifurcation diagrams for the aircraft dynamics in constrained flight maneuvers using the EBA procedure. In the rest of

Received 10 May 2000; revision received 3 January 2001; accepted for publication 5 June 2001. Copyright © 2001 by the American Institute of Aeronautics and Astronautics, Inc. All rights reserved.

*Assistant Professor, Department of Aerospace Engineering; akn@aero.iitb.ac.in; currently Visiting Assistant Professor of Aeronautics, California Institute of Technology, Pasadena, CA 91125; akn@caltech.edu. Member AIAA.

†Ph.D. Student, Department of Aerospace Engineering; nandan@aero.iitb.ac.in.